

PSFC/JA-12-1

**Investigation of the Thomson Scattering-ECE  
Discrepancy in ICRF Heated Plasmas at  
Alcator C-Mod.**

White, A. E., Hubbard, A. E., Hughes, J. W., Bonoli, P. T.,  
Austin\*, M. E., Bader, A., Harvey\*\*, R. W., Lin, Y., Ma, Y.,  
Reinke, M. L.\*\*\*, Wolfe, S. M., Wukitch, S. J.

\* University of Texas, Austin, TX, USA

\*\* CompX, CA, USA.

\*\*\* Oak Ridge Institute for Science and Education (ORISE),  
Oak Ridge, TN, USA

September, 2012

**Plasma Science and Fusion Center  
Massachusetts Institute of Technology  
Cambridge MA 02139 USA**

This work was supported by the U.S. Department of Energy, Grant No. DE-FC02-99ER54512-CMOD. Reproduction, translation, publication, use and disposal, in whole or in part, by or for the United States government is permitted.

# Investigation of the Thomson Scattering-ECE Discrepancy in ICRF Heated Plasmas at Alcator C-Mod

A. E. White<sup>1</sup>, A. E. Hubbard<sup>1</sup>, J. W. Hughes<sup>1</sup>, P. T. Bonoli<sup>1</sup>,  
M. E. Austin<sup>2</sup>, A. Bader<sup>1</sup>, R. W. Harvey<sup>3</sup>, Y. Lin<sup>1</sup>, Y. Ma<sup>1</sup>,  
M. L. Reinke<sup>4</sup>, S. M. Wolfe<sup>1</sup>, S. J. Wukitch<sup>1</sup>

<sup>1</sup> Massachusetts Institute of Technology, Cambridge, MA, USA

<sup>2</sup> University of Texas, Austin, TX, USA

<sup>3</sup> CompX, CA, USA

<sup>4</sup> Oak Ridge Institute for Science and Education (ORISE), Oak Ridge, TN, USA

E-mail: whitea@mit.edu

## Abstract.

This paper reports on new experiments at Alcator C-Mod that were performed in order to investigate the long-standing, unresolved discrepancy between Thomson Scattering (TS) and Electron Cyclotron Emission (ECE) measurements of electron temperature in high temperature tokamak plasmas. Ion cyclotron range of frequency (ICRF) heating is used to produce high temperature conditions where the type of TS-ECE discrepancy observed in the past at JET and TFTR should become observable. At Alcator C-Mod, plasmas with  $T_e(0)$  up to 8 keV are obtained using Ion Cyclotron Resonance Heating (ICRH), ICRF mode conversion heating and a combination of the two heating methods in order to explore the hypothesis that the presence of ICRH-generated fast ions may be related to the discrepancy. In all high temperature cases, the TS and ECE measurements of electron temperature agree to within experimental uncertainties. We find no evidence for the type of discrepancy reported at JET and TFTR. These results show that the TS-ECE discrepancy does not depend on high temperatures alone and also that the presence of ICRH-generated fast ions is insufficient to cause the TS-ECE discrepancy.

## 1. Introduction

In optically thick tokamak plasmas, electron temperature measurements made with Thomson Scattering (TS) and Electron Cyclotron Emission (ECE) diagnostics are typically in excellent agreement when  $T_e < 5$  keV. However, some experiments featuring strong neutral beam and ion cyclotron range of frequency (ICRF) auxiliary heating have shown the existence of a clear discrepancy between  $T_e$  measured by TS and ECE when  $T_e > 7$  keV in TFTR [1, 2] and when  $T_e > 5$  keV in JET [3, 4]. There is presently no explanation for the TS-ECE discrepancy that is observed at either JET or TFTR, but it does not appear to be caused by instrumental effects or measurement errors [3]. A potential TS-ECE discrepancy presents a significant challenge for ITER where core electron temperatures above 20 keV are expected and is a primary motivation for the consideration of an oblique ECE instrument for ITER [5, 6]. Understanding the discrepancy has been called the next major advance for ECE [7].

The discrepancy that was observed at TFTR and JET is characterized by ECE measurements of electron temperature that are systematically higher than the TS measurements at high temperatures. The discrepancy increases linearly with increasing temperature, but there is good agreement between the two measurements at low temperatures [3, 6, 8]. Note that differences between TS and ECE  $T_e$  measurements are often observed in tokamak plasmas with strong Electron Cyclotron Resonance Heating (ECRH), Electron Cyclotron Current Drive (ECCD) and Lower Hybrid Current Drive (LHCD). In these cases, the presence of non-thermal electrons can enhance the EC emission above thermal levels. This causes differences between TS and ECE measurements, where  $T_e^{ECE} > T_e^{TS}$ . Such differences are reasonably well understood [9, 10], in contrast to the TS-ECE discrepancies from JET and TFTR, which remain unexplained.

Here we present a brief summary of past work on the TS-ECE discrepancy, in order to provide background and motivation for the experimental conditions explored at Alcator C-Mod.

The TS-ECE discrepancy was first reported for supershot D-T plasmas at TFTR [1], featuring combined NBI and ICRF heating. The discrepancy appeared as a systematic difference between TS and ECE measurements, with ECE measuring temperatures above TS above  $T_e(0) > 7$  keV, but no cause could be identified [2]. The TS-ECE discrepancy has also been observed with NBI-only in TFTR [6]. NBI injection produces fast ions, which over a certain range of parameters transfer energy predominantly to electrons. Because of the potential strong coupling between the fast ions and the bulk electrons, it has been suggested that NBI could cause a distortion of the electron distribution function at low energies, leading to the observed TS-ECE discrepancy [1, 7]. However, there is no proposed mechanism for how this distortion is produced or maintained against collisional relaxation of the distribution function.

Later, the discrepancy was positively identified at JET in plasmas with combined NBI and ICRH, and extensive work was done to show that it was not caused by

instrumental uncertainties, and that it was indeed a real effect [3]. One key aspect of the JET studies were theoretical calculations showing that a distorted electron distribution function could reproduce both the ECE measurements and the TS measurements [11]. On JET, studies with full ECE spectral measurements using a Michelson interferometer showed that the temperature measured from the 2nd harmonic was not in agreement with TS, if a Maxwellian electron distribution function was assumed, but that the temperature measured from 3rd harmonic was in agreement with TS. When a model electron distribution was introduced having a flattening at low-energies (a non-Maxwellian bulk), the effective temperature measured from the modeled 2nd and 3rd harmonics was in agreement, and also, the TS and ECE measurements would also agree [3, 11]. However, it must be emphasized that no physical mechanism has been proposed to explain how a distortion of the electron distribution function near thermal velocities can be sustained with NBI or ICRF auxiliary heating.

Despite the existence of a real (not due to instrumental error or uncertainty) discrepancy at JET and TFTR, is fair to say that the discrepancy may not be a universal feature of high temperature plasmas. This makes predicting its existence in ITER plasmas problematic. Further complicating the issue of the TS-ECE discrepancy is that the discrepancy at JET was observed in hybrid scenarios featuring combined NBI and ICRH in the years 2001 and 2004 but the discrepancy was not reproduced in experiments in the year 2006 featuring similar plasma conditions [4, 8]. One difference between these two sets of discharges identified by the JET team is the hydrogen minority concentration. In the plasmas where the discrepancy was observed, the hydrogen concentration was low, 3%, and when the discrepancy was not observed, the hydrogen fraction was higher, 8% [8]. The effective tail temperature of ICRH-generated fast ions is very sensitive to the minority fraction, and for low hydrogen fractions on JET, the tail temperature can be very high, exceeding  $T_{eff} = 500$  keV [8, 12, 13]. The observation that the JET TS-ECE discrepancy is correlated with very high-energy ion tails in the plasmas, suggested that the fast ions may play a role in causing the discrepancy [3, 4, 8]. Further work has gone into diagnosing the presence of the non-Maxwellian bulk at JET. For example, recently a new oblique ECE system was deployed at JET [14]. The authors examined a variety of high temperature plasmas with fast-ion populations (NBI-only and NBI+ICRH, with  $T_e(0) < 7$  keV) and found no evidence of deviation from Maxwellian behavior in the data, using both the radial and oblique views. [14].

Even with the non-universality of the TS-ECE discrepancy, this issue has motivated an oblique ECE system for ITER, to constrain the electron temperature measurements in the presence of even a slightly non-Maxwellian bulk [6]. It is therefore very important that current tokamak experiments explore the discrepancy: first to verify the general existence conditions as guided by TFTR and JET cases, and then ideally, to identify the cause of the discrepancy and correct for it.

Alcator C-Mod is a high-performance, compact, high-field diverted tokamak ( $R = 0.67$  m,  $a = 0.22$  m,  $2.5$  T  $< B_T < 8$  T,  $n_e < 3 \times 10^{20} m^{-3}$ ,  $T_e(0) \leq 8$  keV,  $1.2 < \kappa < 1.8$ ) featuring ICRF as the primary auxiliary heating system. Experiments at Alcator C-Mod

can be used to study the correlation between the TS-ECE discrepancy and the presence of ICRH-generated fast ions in the plasma. At Alcator C-Mod, experiments were carried out to produce high temperature conditions with significant ICRH-generated fast ions, and also for comparison, to produce high temperature conditions without ICRH-generated fast ions. It is in plasmas with ICRH-generated fast ions that the JET TS-ECE discrepancies appear, and the JET work has served as the main motivation for the present experiments [3, 4, 8].

The results of the C-Mod experiments are that for all plasmas to date with  $T_e(0) < 8$  keV, we find that TS and ECE measurements are in agreement, to within experimental uncertainties. We find no experimental evidence for the types of disagreement between TS and ECE that was reported on JET and TFTR. The C-Mod result shows that high temperatures alone are not the cause of the discrepancy, consistent with past results from [3, 4, 8]. At Alcator C-Mod, with hydrogen minority ICRH, effective tail temperatures of the fast ion distribution function can be similar to those at JET. The ratio of fast ion slowing down time to an electron distribution function relaxation time is also the same. Since no TS-ECE discrepancy is observed at C-Mod in plasmas with ICRH-generated fast ions, it indicates that the presence of fast ions may be unrelated to the cause of the observed TS-ECE discrepancy at JET, or at least that their presence is not a sufficient condition. These experimental results from C-Mod motivate new experiments at other tokamaks to revisit the TS-ECE discrepancy, and also motivate new modeling and simulation work to explore possible causes of the TS-ECE discrepancy due to NBI.

## 2. Experimental set-up

Three separate ECE instruments are used in this experiment: a 9-channel ECE grating polychromator (GPC-1) [15], a 19-channel ECE grating polychromator (GPC-2) [16, 17], and an ECE Michelson interferometer [18]. The GPC instruments are tuned to measure 2nd harmonic X-mode EC emission. The Michelson interferometer is absolutely calibrated, and the two grating polychromators are cross calibrated to the Michelson interferometer over a wide frequency range. All ECE systems share the same optics and view the plasma perpendicularly at the midplane from the low field side (i.e. none of the views are oblique). The Thomson Scattering (TS) diagnostic used in this experiment is described in Ref. [19]. The lasers are directed vertically into the plasma and the spectra are measured from the outboard midplane. The TS diagnostic features an upgraded polychromator with filter arrangement that can reliably measure temperatures up to  $T_e = 20$  keV [19]. Analysis of the TS measured spectrum assumes that the electron distribution is thermal; that is, the spectral data are fit to a Maxwellian distribution to extract electron temperature.

There are two primary ICRF heating configurations used at C-Mod: hydrogen minority ICRH (fast ions transfer energy to plasma via electron drag and collisions with thermal ions) and mode conversion heating (direct electron Landau damping of the mode converted fast wave). Details of the ICRF systems at C-Mod and physics basis of

each heating method are reviewed in Ref. [20]. We also note that C-Mod has a Lower Hybrid (LH) system [20], but for the experiments reported here, LH is not used.

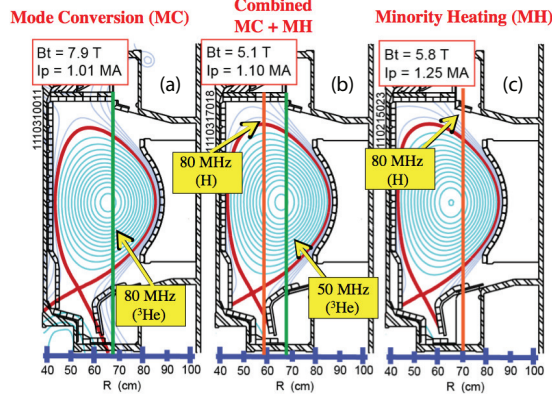


**Figure 1.** (Colour online) Three RF configurations are illustrated: (a) mode conversion (b) combined minority heating and mode conversion and (c) minority heating. The mode conversion layer is near 80 MHz in (a) and near 50 MHz in (b). The Hydrogen resonance layer is at 80 MHz in (b) and (c).

Plasmas in the experiment are all sawtoothing L-mode and I-mode discharges [21], with  $\langle n_e \rangle = 0.9 - 1.5 \times 10^{20} \text{ m}^{-3}$ ,  $P_{RF} = 2 - 5 \text{ MW}$ , and  $I_p = 1.0 - 1.3 \text{ MA}$ . There are three different RF configurations used. In the first heating configuration, Mode Conversion ICRF heating is done by running two species plasmas D( $^3\text{He}$ ) at  $B_t = 7.8 - 8.0 \text{ T}$ , with two antennas set to 80.5 MHz and 80.0 MHz; and a third antenna set to 78.0 MHz. High  $^3\text{He}$  minority fractions (10-15%, scanned shot by shot) are used so that a large percentage of the wave power is mode converted and only a small percentage is absorbed by the minority ions. In this configuration, shown in Figure 1 (a), the mode conversion layer (green) is close to the magnetic axis. In the second configuration, a combination of mode conversion and minority heating can be accomplished by running three species plasmas D(H,  $^3\text{He}$ ) at  $B_t = 5.0 - 5.8 \text{ T}$ . Here two antennas are set to 80.5 MHz and 80.0 MHz, with the third set to 50 MHz. This configuration is shown in Figure 1 (b), where the mode conversion layer (green) is close to the magnetic axis and the Hydrogen resonance layer (orange) is off-axis, on the high field side. In these cases the Hydrogen minority fraction is  $\approx 4 - 6\%$  and the Helium fraction is  $> 15\%$ . In the third configuration, shown in Figure 1 (c), minority heating is done in a two species plasmas D(H) at  $B_t = 5.4 - 5.8 \text{ T}$ . In this case, two antennas are again set to 80.5 MHz and 80.0 MHz, with the third antenna set to 78.0 MHz. At 5.8 T, the Hydrogen resonance layer (orange) is off-axis, on the low field side. The Hydrogen minority fraction is  $\approx 4 - 6\%$ . For all the ICRH plasmas considered here, the critical energy is  $W_{crit} \approx 13.5T_e$  so that fast ions generated in the minority heating configuration slow down predominantly due to electron drag.

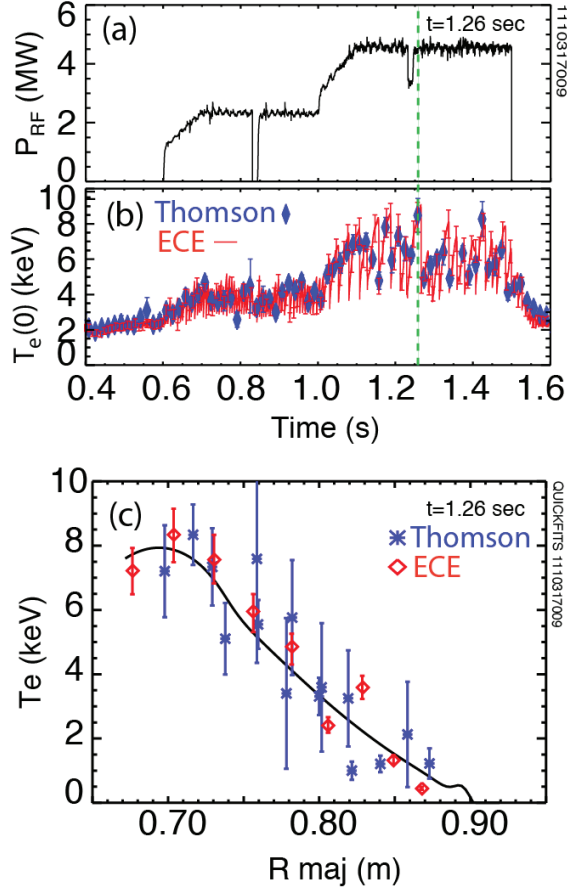


**Figure 2.** (Colour online) (a) Time trace of RF power, (b) central TS (blue-diamond) and ECE data from GPC-1 (red-line) as a function of time, and (c) the electron temperature profile at  $t = 1.26$  s for a high temperature plasma featuring combined mode conversion and minority heating. In (c), TS data are blue asterisks, ECE data are red diamonds.

### 3. Experimental results

Shown in Figure 2 is data from a high temperature plasma featuring both RF mode conversion and minority heating: (a) time trace of RF power, (b) central TS and ECE data (from GPC-1) as a function of time, and (c) the electron temperature profile at  $t = 1.26$  s. Figure 2 (b) shows that there is excellent agreement between the central TS and ECE (GPC-1) measurements at all times in the discharge: during the Ohmic phase before RF is turned on,  $t < 0.6$  sec, with 2.5 MW RF power (mode conversion heating) at low temperatures,  $T_e(0) < 5$  keV, between  $0.6 < t < 1.0$  sec, and with 4.5 MW RF power (combined mode conversion and minority heating) at high temperatures,  $T_e(0) > 5$  keV, between  $1.0 < t < 1.5$  sec.

In order to compare the TS and ECE data points one-to-one, we use data from both GPC-1 and GPC-2. The TS data sets the time base for the TS-ECE comparisons, since the TS data are acquired every 16 ms and the GPC-1 and GPC-2 data are acquired every  $50 \mu\text{s}$ . The ECE data are averaged over 1 ms at the time of comparison. As can be seen

in Figure 2 (b), the GPC-1 ECE data (red) track the sawteeth throughout the shot, but due to the slower TS sampling rate the TS data (blue) measure the highest temperature (peak of a sawtooth) less frequently. This limits the number of data points obtained at high temperature that can be used for a one-to-one TS-ECE comparison in any single discharge. Also, the large (multi-keV) sawteeth crashes occurring during interferograms can lead to spurious structure in the measured profiles. For these reasons, the slowly scanning Michelson interferometer data were not used to investigate the discrepancy: there were too few spectra measured at the high temperature times to form a complete data set. At low temperatures, there is excellent agreement between the TS, GPC, and 2nd harmonic Michelson profiles.

There are six TS-ECE pairs used in the comparisons, since three TS channels overlap in radius with three GPC-1 channels and three GPC-2 channels. A data pair is made up of the TS data point and the ECE data point that are nearest to one another spatially. The pairs are located at radii of  $R = 0.68, 0.70$  and  $0.72$  m, where we label the location of the pair based on the radial location of the TS data point. For each pair, the TS measurement location is separated from the ECE measurement position always by less than 1 cm, with the separation between TS and ECE measurement locations ranging between  $\pm 0.3$  cm and  $\pm 0.8$  cm for each pair.

Figure 2 (c) shows the electron temperature profile data plotted versus major radius. The Thomson data (blue) and ECE data (red) are in good agreement. The black solid line is a fit to the data shown and the edge TS data (not shown). Experimental error bars on the measured temperature are shown. The TS data are mapped from real space into flux coordinates via EFIT [22] and are then compared with the GPC data, which are also mapped from real space into flux coordinates using the EFIT reconstruction. Errors in radial mapping near the magnetic axis due to uncertainties in the equilibrium reconstruction are estimated to be between 1.0 cm and 1.5 cm. The ECE data are mapped using the cold resonance location, which means that due to relativistic broadening, the ECE sample volume extends 1.0 – 1.5 cm in the radial direction on the high field side of the data points shown in the temperature profile. The ECE sample volume near the magnetic axis has a vertical extent of roughly 4 cm due to the GPC antenna pattern. The spatial resolution of the TS diagnostic is subcentimeter: a few mm in the radial direction with a vertical extent of the scattering volume  $\sim 6$  mm at the center of the plasma. All the discharges in this study are relatively low density discharges for C-Mod ( $\langle n_e \rangle < 1.5 \times 10^{20} \text{ m}^{-3}$ ), and error bars on TS are atypically large (Figure 2) because of the reduced signal to noise.

The TS-ECE comparison results from all three heating configurations are summarized in Figure 3. Central temperature measured with ECE (using both GPC1 and GPC2 data) is plotted on the vertical axis and central temperature measured with Thomson Scattering is plotted on the horizontal axis. All pairs of ECE and TS data from within the radial range  $0.68 \text{ m} < R_{maj} < 0.72 \text{ m}$  near the magnetic axis are plotted. We restrict the comparison to pairs of TS and ECE measurements made within 1 ms of each other, and separated in radius by less than 1 cm. There are over 600 TS-ECE data pairs



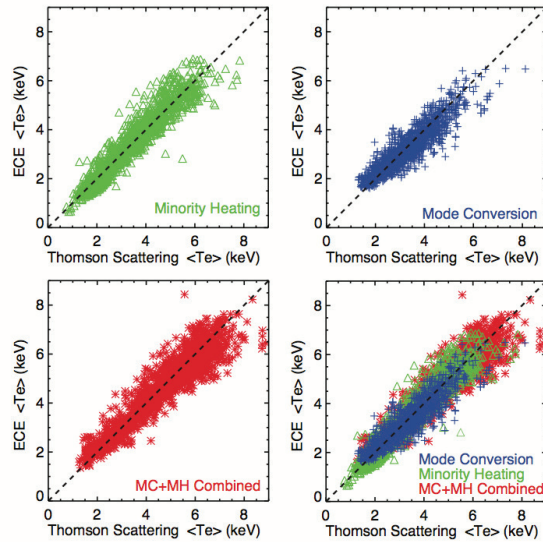


**Figure 3.** (Colour online) Central temperature measured with ECE (using both GPC1 and GPC2 data) compared with Thomson Scattering. All pairs of ECE and TS data from within the radial range  $0.68 \text{ m} < R_{maj} < 0.72 \text{ m}$  are plotted. The paired measurements are made within 1 ms of each other, and are separated in radius by less than 1 cm

from the mode conversion cases (blue-diamonds) taken from 14 discharges, over 1600 data pairs for minority heating (green-triangles) cases taken from 14 discharges, and over 3200 data pairs for combined mode conversion and minority heating (red-asterisks) cases taken from 20 discharges. The black-dashed line indicates the unity line; it is not a regression line or fit to the data.

Plotting the data in the format of Figure 3 shows qualitatively that there appears to be no gross systematic difference between the two measurements over the temperature range  $1.5 < T_e < 8.0 \text{ keV}$ . From this figure, there is already evidence that the type of TS-ECE discrepancy seen at JET and TFTR is not present in the C-Mod data. For the TS-ECE discrepancy on JET and TFTR, the TS and ECE data would begin to disagree outside error bars only at higher temperature, while agreeing within error bars at lower temperature. Figure 3 does show that the scatter in the data about the unity line increases with increasing temperature, but it also shows that there is no trend for ECE measurements to be higher than TS measurements at higher temperature. This scatter plot analysis is useful in general for identifying calibration errors on a channel by channel basis. We were able to identify one data pair where the TS temperature was systematically higher than the ECE temperature on two of the experimental run days; we note that this difference was present at both low and high temperatures and is unrelated to the TS-ECE discrepancy of interest.

A statistical model is used to compare measurements from each instrument quantitatively to determine if any evidence for the TS-ECE discrepancy exists [23, 24, 25]. The model can be used to quantify differences between the two instruments directly

as long as the instrumental effects are constant at all temperatures and that the between instrument bias is constant at all temperatures. For the C-Mod data, Figure 3 suggests that the second assumption is well-satisfied, but Figure 3 also shows that scatter in the data from one or both instruments increases as temperature increases, and this will need to be later taken into account by log-transforming the data, which is discussed later in this section.

The TS and ECE measurements are made at a series of times during the discharge, with each measurement in time denoted with  $i$ . The temperature measurement from each instrument can be expressed as the sum of the true (but unknown) electron temperature at each time,  $T_i$ , plus average random error,  $\epsilon_i$ , plus average bias error,  $\beta_i$ . That is, we have  $T_{ECE,i} = T_i + \epsilon_{ECE,i} + \beta_{ECE,i}$  and  $T_{TS,i} = T_i + \epsilon_{TS,i} + \beta_{TS,i}$ , for the ECE and TS measurements, respectively.

The TS and ECE measurements will agree if the average random error and the average bias error are the same. Standard tests exist to determine if  $\epsilon_{TS} = \epsilon_{ECE}$  and if  $\beta_{TS} = \beta_{ECE}$  [23, 24, 25, 26, 27]. Here we follow the analysis of Ref. [24], and we form Bland-Altman test plots to assess the level of agreement between the TS and ECE measurements. The Bland-Altman test consists of a plot of the difference between the two measurements versus the mean of the two measurements. By plotting the difference between the two measurements against their mean, we assess whether or not the random errors and average measurement biases are the same for the two measurement methods. The average of the two measurements  $(T_{ECE,i} + T_{TS,i})/2$  represents our best guess of the true (but unknown) temperature, and we define  $d_i$  the difference between two measurements  $d_i = T_{ECE,i} - T_{TS,i}$ . Shown in Figure 4 are the Bland-Altman plots for each heating configuration: (a) mode conversion, (b) minority heating and (c) combined mode conversion and minority heating. The black dashed line is at  $d = 0$ , the green dashed line is the average of the differences from  $n$  measurements,  $\langle d \rangle = \frac{1}{n} \sum_{i=1}^n d_i$ . The red dashed lines are drawn at  $\langle d \rangle \pm 2\sigma$ , where the standard deviation is defined by  $\sigma^2 = \frac{1}{n-1} \sum_{i=1}^n (d_i - \langle d \rangle)^2$

Figure 4 is a visual analog of the test of the product moment correlation [25], and can be used to test the hypothesis that  $\epsilon_{TS} = \epsilon_{ECE}$ . Since the data in Figure 4 show little trend in the difference with respect to the mean, we conclude that  $\epsilon_{TS} \approx \epsilon_{ECE}$ . The average difference,  $\langle d \rangle$  is an unbiased estimate of the difference in the average measurement biases,  $\beta_{TS} - \beta_{ECE}$ . For all three heating configurations cases shown in Figure 4, difference in measurement biases is small, but is not zero. So we reject at the 100% confidence level the hypothesis that  $\beta_{TS} = \beta_{ECE}$ .

Because the scatter in the TS and ECE measurements increases with temperature, it is not possible to directly use the difference plots from Figure 4 to quantify the bias and error in the measurements. Instead, log transformed difference plots, like those shown in Figure 5, are used to extract quantitative estimates of the level of agreement between the TS and ECE measurements [23].

From Figure 5 (a), we compare measurements for the mode conversion cases. The mean difference is -0.04 on the log scale and the limits of agreement are -0.12

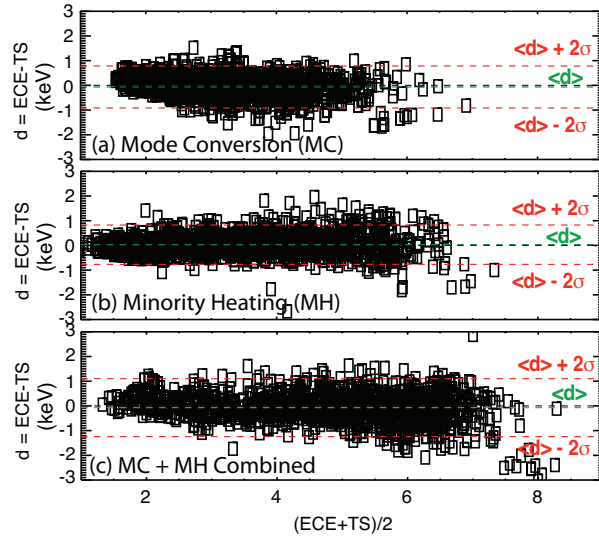


**Figure 4.** (Colour online) Bland-Altman plots for each heating configuration: (a) mode conversion, (b) minority heating and (c) combined mode conversion and minority heating

and 0.11, and the antilog of these limits gives 0.76 and 1.29, respectively. This gives the dimensionless ratio that represents the percent difference between the ECE measurements and the TS measurements, that is, these limits tell us that for 95% of the mode conversion cases compared, the ECE measurement will differ from the TS measurement by 24% below to 29% above. The bias of the ECE is roughly 9% below TS in the mode conversion RF heating cases. Performing the same calculations for the minority heating cases shown in Figure 5 (b), we find that for 95% of the cases compared, the ECE measurement will differ from the TS measurement by 21% below to 29% above, with ECE biased above TS by 1%. For the combined mode conversion and minority heating cases shown in Figure 5 (c), we find that for 95% of the cases compared, the ECE measurement will differ from the TS measurement by 22% below to 29% above, with ECE biased below TS by 5%. In Figure 4 and Figure 5, we plot all data pairs together in order to compare the three different heating configurations. Plots made for each channel pair give similar results.

In order to connect to the past TS-ECE discrepancy work at JET and TFTR [6, 8], it is the average instrument biases that are of interest, and how these vary with temperature. The manifestation of the JET and TFTR TS-ECE discrepancy is that ECE is biased above TS at high temperatures, but has a similar bias at low temperatures. For the C-Mod cases, we find that ECE measurements of  $T_e$  are biased higher than the TS measurements by 1% in the best case, the MH configuration shown in Figure 5 (c), and are biased below the TS measurements by 9% in the worst case, the MC configuration shown in Figure 5 (a). We find that the difference in average instrument biases is independent of temperature. From Ref. [8], the reported discrepancy gave ECE measurements higher than TS measurements by 15 – 20%, outside experimental

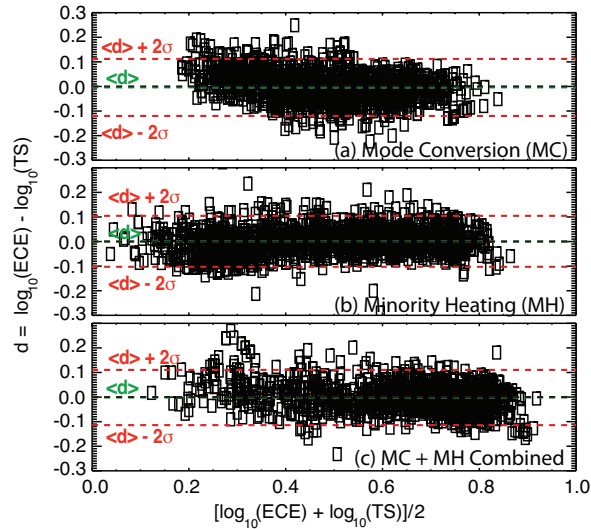


**Figure 5.** (Colour online) Log transformed difference plots for each heating configuration: (a) mode conversion, (b) minority heating and (c) combined mode conversion and minority heating

uncertainties, at high temperature only. In contrast, for the C-Mod cases, the difference in biases is between 1% and 9%, which is acceptable given the desired measurement accuracy, (i.e. 10%). We also note that the three scenarios used different magnetic fields, so the GPC is measuring different frequency ranges in each case. Thus data sets from each scenario may have different systematic and calibration uncertainties. Overall, the experimental data from C-Mod show no evidence for the type of discrepancy that was observed at TFTR and JET.

#### 4. Possible role of fast ions for the TS-ECE discrepancy

At JET, the data showed that ECE measurements were systematically higher than TS at high temperatures in hybrid scenario discharges with combined neutral beam injection (NBI) and ion cyclotron resonant heating (ICRH) [3, 4, 8]. It has been established that the discrepancy at JET is correlated with low hydrogen minority concentrations, and is therefore only observed in discharges with a very high-energy ion tail caused by ICRH [3, 4, 8]. At C-Mod, there is no evidence of the TS-ECE discrepancy in any heating configuration, with or without fast ions, so we cannot directly compare with the JET results. Of course there is the possibility that differences in the ICRH-generated fast ion populations in the two tokamaks might cause the TS-ECE discrepancy to appear at JET, but not at C-Mod. We consider two parameters to compare the JET and C-Mod results: effective fast ion tail temperature and the ratio of fast ion slowing down time to an electron energy distribution function relaxation time. If there were a mechanism by which fast ions could perturb the electron distribution function, it is reasonable to assume that it would depend on the fast ion slowing down time and effective fast ion tail temperature, which play a role in determining how fast ions transfer energy and

momentum to electrons [28, 29].

For these experiments, the fast ion spectrum is measured via passive charge exchange with the Compact Neutral Particle Analyser (CNPA) [30, 31]. The CNPA data provides information on the fast proton density at energies between 0.1 – 1.0 MeV and the spectrum is fit to an exponential in order to extract an effective fast ion tail temperature using simple models [30, 31]. Absolute energies of the fast ions on JET can be much higher than those on C-Mod due to the lower plasma density at JET,  $n_e \sim 1 \times 10^{19} \text{ m}^{-3}$ , compared to C-Mod ( $n_e \sim 1 \times 10^{20} \text{ m}^{-3}$ ). However, the measured effective fast ion tail temperatures for the C-Mod Hydrogen minority heating cases considered in this paper range from  $0.2 < T_{eff} < 0.5 \text{ MeV}$ , which are similar to those reported in JET [12, 13]. This can be understood by considering that the effective tail temperature, the slowing down time, and the minority ion density determine the rate of power transfer from the fast ions to the background plasma (i.e. an RF power density). Due to the larger volume of JET compared to C-Mod, the RF power density in C-Mod is  $\approx 100$  times larger for the same input RF power. Using JET plasma parameters from Refs. [12, 13], the fast ion slowing down time is  $\tau_s \approx 2 \text{ s}$ , compared to  $\tau_s \approx 0.2 \text{ s}$  at C-Mod. For the same D(H) minority heating configuration (same hydrogen minority fraction and plasma temperature), due to the differences in plasma density and RF power density between JET and C-Mod, the effective fast ion tail temperatures at the two tokamaks are expected to be the same. This is confirmed by the CNPA measurements in the C-Mod experiments.

Past modeling on the TS-ECE discrepancy showed that a depletion of low velocity electrons that leads to a flattening of the electron distribution function can explain the JET discrepancy [8, 11]. It is of interest to estimate how fast such distortions at low energies and velocities relax due to electron-electron collisions. As noted previously, collisions should very efficiently maintain a Maxwellian bulk of the distribution function, assuming there is no resonant wave particle interaction driving anisotropy [6]. The energy exchange time,  $\tau_{ee} = 1/\nu_{ee}$ , is the typical time required for the electron distribution function to approach a Maxwellian distribution. For the C-Mod experiments  $\tau_{ee} \approx 150 \mu\text{s}$  at  $T_e = 8 \text{ keV}$ , and for JET parameters [12, 13]  $\tau_{ee} \approx 1.0 - 1.5 \text{ ms}$  at  $T_e = 8 \text{ keV}$ . For both tokamaks,  $\tau_{ee}$  is three orders of magnitude smaller than the fast ion slowing down time, which indicates that from a collisional standpoint, the distribution function will relax to a Maxwellian much faster than the energetic ions can modify the electron distribution function.

## 5. Conclusions

Experiments using ICRF heating were carried out at Alcator C-Mod to investigate the TS-ECE discrepancy in high temperature plasmas,  $T_e(0) \leq 8 \text{ keV}$ . Plasmas from three different run-days with three different heating configurations with high temperatures of  $T_e(0) \leq 8 \text{ keV}$  are used for the one-to-one comparison of TS and ECE data. We have found no evidence of the type of TS-ECE discrepancy observed at JET and TFTR.

The TS and ECE measurements of electron temperature are found to agree to within experimental uncertainties at low and high temperatures. Disagreements between TS and ECE measurements that are observed can be attributed to random errors and systematic errors, e.g. in the calibration of one or both instruments.

These results from C-Mod provide new and valuable information regarding the TS-ECE discrepancy seen at JET and TFTR. First, since the C-Mod data cover the same temperature range,  $T_e > 5$  keV, where the JET discrepancy was observed [3, 4, 8], this is new experimental evidence suggesting that the presence of the discrepancy cannot depend on high temperature alone. This supports the JET results [3, 4, 8]. Second, the minority heating configuration on C-Mod is the same ICRF heating method used at JET for the TS-ECE discrepancy cases studied [4, 8]. Since parameters that determine how the ICRH-generated fast ions transfer energy and momentum to the electrons (effective tail temperature and the ratio  $\tau_s/\tau_{ee}$ ) are the same in both JET and C-Mod there appears to be no obvious reason why JET data should exhibit a discrepancy but not C-Mod. This suggests that the TS-ECE discrepancy seen on JET, while correlated with the presence of energetic ions, may not be caused by the energetic ions. Certainly, the presence of fast ions is not sufficient to cause a discrepancy in the C-Mod cases examined. Future modeling work using Fokker-Planck codes such as CQL3D [33] to self-consistently evolve the electron distribution function and the fast ion distribution function simultaneously in order to probe the physics of how fast ions affect the electron distribution function could help shed more light on the possible effects of fast ions.

New experiments on all tokamaks should be carried out at high temperature to further investigate the causes of the TS-ECE discrepancies that exist in the JET and TFTR data. In particular, new experiments at DIII-D are planned to explore causes of the TFTR discrepancy in neutral beam heated cases. Future experiments to investigate the discrepancy should include, when possible, measurements of (or at least constraints on) the electron temperature using diagnostics other than TS and ECE. One example would be exploiting relativistic effects to extract  $T_e$  from reflectometry measurements [34] or perhaps using a spatially resolving, spherically bent x-ray crystal spectrometer to assess  $T_e$  from impurity lines [35]. Since high temperature plasmas  $T_e(0) > 8$  keV can be obtained relatively routinely now at C-Mod in the I-mode regime [21], it will be possible to continue to add to the existing database that was analyzed for this paper. In particular, expanding the MC data set from C-Mod will be pursued, as well as experiments to probe temperatures above 8 keV in C-Mod. The discrepancy may appear at higher temperatures than those accessed in the present experiments. It would also be useful to re-examine and compare databases from C-Mod, TFTR and JET in order to look for scalings the TS-ECE discrepancy may have with respect to plasma density, plasma size, or power density in ICRH plasmas.

## Acknowledgments

We thank the Alcator C-Mod team for their support of the measurements reported here. AEW gratefully acknowledges E. de la Luna, R. Prater and C. C. Petty for their insights on probing the TS-ECE discrepancy and B. Bray for helpful discussions of errors and uncertainty in TS measurements. This work supported by the US Department of Energy under DE-FC02-99ER54512.

## References

- [1] G. Taylor and et al. Electron cyclotron emission measurements on high beta TFTR plasmas. *Proc. 9th Joint Workshop on ECE and ECRH (Borrego Springs, USA, 1995) ed. J. LOHR (World Scientific, Singapore, 1995)*, page 485, 1995.
- [2] I. Fidone, G. Giruzzi, and G. Taylor. Plasma diagnostics in the Tokamak Fusion Test Reactor using emission of electron cyclotron radiation at arbitrary frequencies. *Physics of Plasmas*, 3:2331, 1996.
- [3] E. de la Luna, V. Krivenski, G. Giruzzi, C. Gowers, R. Prentice, J. M. Travere, and M. Zerbini. Impact of bulk non-maxwellian electrons on electron temperature measurements (invited). *Rev. Sci. Instrum.*, 74:1414–1420, 2003.
- [4] K. V. Beausang, S. L. Prunty, R. Scannell, M. N. Beurskens, M. J. Walsh, E. de la Luna, and JET EFDA Contributors. Detecting non-maxwellian electron velocity distributions at JET by high resolution Thomson scattering. *Rev. Sci. Instrum.*, 82:033514, 2011.
- [5] E. de la Luna and JET-EFDA contributors. Physics of ECE temperature measurements and prospects for ITER. volume 988, pages 62–72. AIP Conference Proceedings, 2007.
- [6] G. Taylor and R. W. Harvey. Assessment of an oblique ECE diagnostic for ITER. *Fusion Science and Technology*, 55:64, 2009.
- [7] A. Costley. ECE: The story so far. *Proc. 15th Joint Workshop on ECE and ECRH (Yosemite, USA, 2008) ed. J. LOHR (World Scientific, Singapore, 2008)*, page 3, 2008.
- [8] E. de la Luna and et al. Recent results on the discrepancy between electron temperature measurements in high temperature plasmas in JET. *Proc. 15th Joint Workshop on ECE and ECRH (Yosemite, USA, 2008) ed. J. LOHR (World Scientific, Singapore, 2008)*, page 123, 2008.
- [9] V. Krivenski. Electron cyclotron emission by non-maxwellian bulk distribution functions. *Fusion Engineering and Design*, 53:23, 2001.
- [10] S Coda, I Klimanov, S Alberti, G Arnoux, P Blanchard, A Fasoli, and the TCV team. The effect of ECRH on the electron velocity distribution function. *Plasma Physics and Controlled Fusion*, 48(12B):B359, 2006.
- [11] V. Krivenski, E. de la Luna, and G. Giruzzi1. Evidence of non-maxwellian electron bulk distributions on JET. *29th EPS Conference on Plasma Phys. and Contr. Fusion Montreux, 17-21 June 2002, ECA*, 26B(O):1.03, 2002.
- [12] V. G. Kiptily and et al.  $\gamma$ -ray diagnostics of energetic ions in JET. *Nuclear Fusion*, 42:999, 2002.
- [13] V. G. Kiptily and et al. Recent progress in fast ion studies on JET. *Nuclear Fusion*, 49:065030, 2009.
- [14] L. Figini, S. Garavaglia, E. De La Luna, D. Farina, P. Platania, A. Simonetto, C. Sozzi, and JET-EFDA Contributors. Measure of electron cyclotron emission at multiple angles in high Te plasmas of JET. *Review of Scientific Instruments*, 81(10):10D937, 2010.
- [15] P. J. O’Shea, A. E. Hubbard, and the Alcator C-Mod Group. Nine channel polychromator for fast  $t_e$  measurements on Alcator C-Mod. *Proc. 9th Joint Workshop on ECE and ECRH (Borrego Springs, USA, 1995) ed. J. LOHR (World Scientific, Singapore, 1995)*, page 7, 1995.
- [16] A. Janos and et al. Operation of two grating polychromators on TFTR and new observations of magnetohydrodynamic phenomena. *Rev. Sci. Instrum*, 66:668, 1995.

- [17] G. Taylor and et al. Electron power deposition measurements during ion cyclotron range of frequency heating on C-Mod. *AIP Conf. Proc.*, 485:490, 1999.
- [18] T. C. Hsu, S. E. Kissel and I. H. Hutchinson. A novel fast scan Michelson interferometer for ECE diagnostic applications on Alcator C-Mod. *Proceedings of the 7th Joint Workshop and IAEA Technical Committee on Electron Cyclotron Emission and Electron Cyclotron Resonance Heating*, (Hofei, China) (Vienna: IAEA) p. 31, 1990.
- [19] J. W. Hughes, D. Mossessian, K. Zhurovich, M. DeMaria, K. Jensen, and A. Hubbard. Thomson scattering upgrades on Alcator C-Mod. *Review of Scientific Instruments*, 74(3):1667–1670, 2003.
- [20] P. T. Bonoli and et al. Wave-particle studies in the ion cyclotron and lower hybrid ranges of frequencies in Alcator C-Mod. *Fusion Science and Technology*, 51:401, 2007.
- [21] D.G. Whyte, A.E. Hubbard, J.W. Hughes, B. Lipschultz, J.E. Rice, E.S. Marmor, M. Greenwald, I. Cziegler, A. Dominguez, T. Golfinopoulos, N. Howard, L. Lin, R.M. McDermott, M. Porkolab, M.L. Reinke, J. Terry, N.Tsujii, S. Wolfe, S. Wukitch, Y. Lin, and the Alcator C-Mod Team. I-mode: an H-mode energy confinement regime with L-mode particle transport in Alcator C-Mod. *Nuclear Fusion*, 50(10):105005, 2010.
- [22] L.L. Lao, H. St. John, R.D. Stambaugh, A.G. Kellman, and W. Pfeiffer. Reconstruction of current profile parameters and plasma shapes in tokamaks. *Nucl. Fusion*, 25(11):1611, 1985.
- [23] D. G. Altman and J. M. Bland. Measurement in medicine: The analysis of method comparison studies. *Journal of the Royal Statistical Society. Series D (The Statistician)*, 32(3):307, 1983.
- [24] D. G. Altman and J. M. Bland. Statistical methods for assessing agreement between two methods of clinical measurement. *Lancet*, i:307, 1986.
- [25] A. Kinsella. Estimating method precisions. *Journal of the Royal Statistical Society. Series D (The Statistician)*, 35(4):421, 1986.
- [26] Gerald J. Hahn and Wayne Nelson. A problem in the statistical comparison of measuring devices. *Technometrics*, 12(1):95, 1970.
- [27] Frank E. Grubbs. Errors of measurement, precision, accuracy and the statistical comparison of measuring instruments. *Technometrics*, 15(1):53, 1973.
- [28] T. Stix. Fast-wave heating of a two-component plasma. *Nuclear Fusion*, 15:737 754, 1975.
- [29] G. Hammett. Fast ion studies of ion cyclotron heating in the PLT tokamak. *PhD dissertation, Princeton, Department of Astrophysical Science*, 1986.
- [30] V. Tang et al. Compact multichannel neutral particle analyzer for measurement of energetic charge-exchanged neutrals in Alcator C-Mod. *Rev. Sci. Instrum.*, 77:084501, 2006.
- [31] A. Bader, R. S. Granetz, R. R. Parker, P. T. Bonoli, I. H. Hutchinson, J. Sears, and S. J. Wukitch. Experimental measurements of ICRF minority-heated fast-ion distributions on Alcator C-Mod. *submitted for publication to Nuclear Fusion*, December 2011.
- [32] Lyman Spitzer Jr. *Physics of Fully Ionized Gases*. Dover Publications, NY. Unabridged republication of Second Revised Edition published by John Wiley and Sons, 1962, 2006.
- [33] R. W. Harvey and M. G. McCoy. The CQL3D Fokker-Planck code. Proceedings of the IAEA Technical Committee Meeting on Advances in Simulation and Modeling of Thermonuclear Plasmas, Montreal, Canada, p. 527, 1992. Available at USDOC/NTIS doc DE93002962, <http://www.compxco.com/cql3d.html>
- [34] L. Zeng, W. A. Peebles, E. J. Doyle, T. L. Rhodes, and G. Wang. Relativistic effects on reconstruction of density profiles via reflectometry in ITER and potential for electron temperature measurements. *Plasma Phys. Control. Fusion*, 49:12771287, 2007.
- [35] N. Pablant and et al. First results from the high-resolution x-ray imaging crystal spectrometer on the Large Helical Device. In *53rd Annual Meeting of the APS Division of Plasma Physics*, volume 56, 2011.